

Article

Ozone Trends from Two Decades of Ground Level Observation in Malaysia

Fatimah Ahamad ^{1,*}, Paul T. Griffiths ², Mohd Talib Latif ³, Liew Juneng ³ and Chung Jing Xiang ⁴

¹ Centre for Tropical Climate Change System, Institute of Climate Change, Universiti Kebangsaan Malaysia, UKM Bangi 43600, Malaysia

² National Centre for Atmospheric Science, Department of Chemistry, University of Cambridge, Lensfield Road, Cambridge CB2 1EP, UK; paul.griffiths@ncas.ac.uk

³ Department for Earth Sciences and Environment, Faculty of Science and Technology, Universiti Kebangsaan Malaysia, UKM Bangi 43600, Malaysia; talib@ukm.edu.my (M.T.L.); juneng@ukm.edu.my (L.J.)

⁴ Institute of Oceanography and Environment, Universiti Malaysia Terengganu, Kuala Nerus 21030, Malaysia; jingxiang@umt.edu.my

* Correspondence: fatimah.a@ukm.edu.my

Received: 28 June 2020; Accepted: 15 July 2020; Published: 17 July 2020



Abstract: We examine the change in surface ozone and its precursor behavior over 20 years at four locations in western Peninsular Malaysia which have undergone urban-commercial development. Trend and correlation analyses were carried out on ozone and oxides of nitrogen observation data over the periods of 1997–2016 as well as the decadal intervals of 1997–2006 and 2007–2016. Diurnal variation composites for decadal intervals were also plotted. Significant increasing ozone concentrations were observed at all locations for the 20-year period, with a range between 0.09 and 0.21 ppb yr⁻¹. The most urbanized location (S3) showed the highest ozone trend. Decadal intervals show that not all stations record significant increasing trends of ozone, with S1 recording decreasing ozone at a rate of −0.44 ppb yr⁻¹ during the latter decade. Correlation analysis showed that only oxides of nitrogen ratios (NO/NO₂) had significant inverse relationships with ozone at all stations corresponding to control of ozone by photostationary state reactions. The diurnal composites show that decadal difference in NO/NO₂ is mostly influenced by change in nitric oxide concentrations.

Keywords: ozone precursors; long term ozone measurements; gaseous pollutant ratios

1. Introduction

Surface ozone (O₃) is a pollutant that affects human health and crop yields [1–4]. O₃ studies in urban areas, particularly in the urban-commercial hub within and around Kuala Lumpur, the capital city of Malaysia, have shown frequent incidences of high O₃ and other pollutant concentrations such as particulate matter [5–7]. Within the greater Klang Valley conurbation, which is the most densely populated area in Malaysia, surface O₃ exposure has reached levels that pose significant risks to health [4]. However, a study on public perception on air quality in the area indicates that more than two-thirds of respondents did not perceive any threats to their health and have a positive outlook on the air quality status in the area. Concerns on air quality discussed in popular media in Malaysia are typically associated with severe haze episodes caused by large scale biomass burning in the region that causes perceivable reduction in visibility [8,9]. Since O₃ is a colorless gas that does not have a pungent odor, there is likely less awareness of the severity of O₃ pollution when it is not accompanied by haze episodes.

Mitigation and control of O₃ pollution is challenging as it is not a pollutant that is directly emitted into the atmosphere. O₃ is formed through reactions of precursors such as oxides of nitrogen (NO_x) and volatile organic compounds (VOC) that contribute to the formation of atomic oxygen (O). Reaction of this atomic oxygen with molecular oxygen (O₂) results in the formation of O₃. Although O₃ formation from oxygen appears straightforward, O₃ photochemistry is complex. The NO_x pathway of O₃ formation, for example, also involves the destruction of O₃ by nitric oxide (NO), when NO concentrations are sufficiently high [10,11]. In urban environments, O₃ formation can be classified into NO_x-sensitive and VOC-sensitive regimes. In the NO_x-sensitive regime, reducing NO_x will result in greater reduction in O₃ compared to reducing VOC, while the opposite is true for the VOC-sensitive regime [12]. Formation of surface O₃ also requires the presence of sunlight. Hence, its level is strongly influenced not only by the complex chemical pathways involved in its formation and destruction, but also by meteorological factors that drive these reactions [10,13–15].

In Malaysia, studies on surface O₃ pollution have mostly focused on relatively short study periods of ten years or less [16–18]. These studies have explained the relationship between O₃ and its precursors as well as meteorological parameters at diurnal and seasonal scales. The monsoon seasons in Malaysia have been shown to influence the intra-annual variability of O₃ with both local and regional transport associated with seasonal winds influencing O₃ episodes in Malaysia [5,17,19]. Variability of O₃ during high particulate matters events associated with haze and non-haze episodes has also been studied, as O₃ showed a positive relationship with high particulates events at diurnal scale [20,21].

Although the seasonal and diurnal variability of O₃ in Malaysia has been extensively studied, very few studies have focused on determining long term O₃ trends, particularly in the western coast of the peninsula where the Klang Valley is located. A long term study on a background surface O₃ monitoring site showed a positive O₃ trend for the period between 1997 and 2011, associated with expanding anthropogenic activity in the surrounding area [22]. In contrast, daily maximum O₃ trends in Malaysian Borneo showed that only four out of the six available monitoring stations recorded increasing O₃ trends for the period between 2002 and 2013. It would appear that not all locations show consistently increasing trends in O₃ within the country and it is unclear if differences in O₃ trends would directly relate to its precursor trends. Given that Malaysia is a tropical country that has markedly different seasonal weather profile from countries in mid-latitudes and has been undergoing rapid urban expansion since the early 1990s, analyzing its long term O₃ behavior is expected to provide some insight into O₃ behavior in a developing country over the tropical region.

The main aim of this study is to identify O₃ and oxides of nitrogen trends over two decades at four locations in western Peninsular Malaysia that have undergone urban-commercial development. O₃ and precursor trends as well as correlation were determined, and diurnal variation composites for decadal intervals were further plotted to determine the relationship between O₃ and oxides of nitrogen over the periods of 1997–2016, 1997–2006, and 2007–2016. Decadal intervals were also included in the analysis for comparing patterns in O₃ trends to determine if the trends are still consistent when different intervals are analyzed.

2. Data and Methodology

Gaseous pollutant records between 1997 and 2016 at four stations within the Department of Environment (DoE) Malaysia's ambient air quality network were selected and analyzed (Figure 1). Station selection was done based on pollutant data availability for the duration of the study and its location within Peninsular Malaysia. The Malaysian peninsula can be divided into the western, eastern, and southern region as the Titiwangsa mountain range bisects the peninsula from the north to more than two-thirds of Peninsular Malaysia toward the south. The topography influences meteorology such as the difference in seasonal rainfall between the east and west [23]. Western Peninsular Malaysia has more densely populated areas and commercial-industrial zones compared to the east.

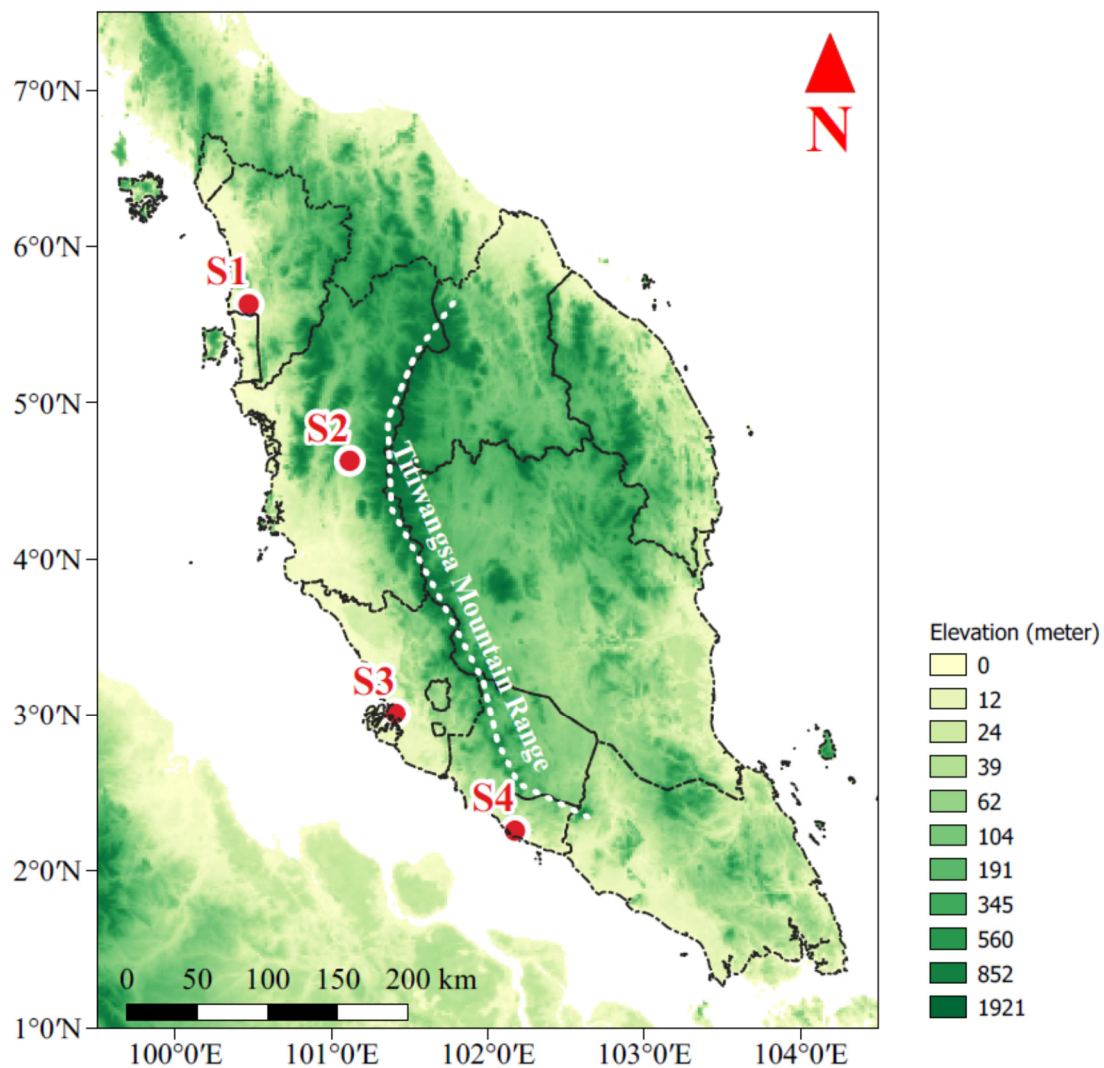


Figure 1. Location of the four monitoring stations within Peninsular Malaysia.

Hourly O_3 measurements were made using a UV absorption O_3 analyzer (Teledyne Model 400A, San Diego, CA, USA). NO and NO_x measurements as well as NO_2 readings were obtained from the Teledyne Model 200A analyzer (San Diego, CA, USA). Carbon monoxide (CO) measurements were taken using a Teledyne Model 300 analyzer (San Diego, CA, USA). Sulphur dioxide (SO_2) measurements were made using Teledyne Model 100A/E (San Diego, CA, USA). Additional information on instruments can be found in Latif et al. (2014) [22]. For the period between 1997 and 2016, the DoE contracted the measurements of pollutants and the calibration of equipment for the continuous air quality monitoring network to Alam Sekitar Malaysia Sdn. Bhd. Calibration and maintenance schedules include daily autocalibration for all pollutants and monthly maintenance. Data transferred to the DoE used here are data that have undergone calibration and maintenance schedules that were designed based on United States Environmental Protection Agency standards.

Data from the DoE were preprocessed to discard zero readings for pollutant concentration, and no computational method was used to replace or impute hourly missing value for the pollutants. To reduce the impact on data homogeneity, if large continuous missing values were present in O_3 data, only stations that recorded 10% or less hourly missing data within the 20-year period were selected. These were then further checked to determine that no more than 25% of these hourly data were missing each year. For all other pollutants, the total missing value had to be less than 30%, while the annual missing value had to be less than 50% to fulfil station selection criteria. The 50% cut-off is deemed acceptable, given that Malaysia is a tropical country without large seasonal variability such as those

observed in mid latitudes. A similar cut-off point has also been employed in a Hong Kong study on long term O₃ trends [24]. Information on station location and data availability is presented in Table 1. Missing values for the monthly data are visually represented in the time series plots shown and discussed in Section 3 (Figures 4 and 6).

Table 1. Station location and data availability.

Station ID	S1	S2	S3	S4	
Location	Sungai Petani, Kedah	Tasek Ipoh, Perak	Klang, Selangor	Bukit Rambai, Melaka	
Latitude (°N)	5.6314	4.6297	3.0103	2.2585	
Longitude (°E)	100.47	101.11	101.40	102.17	
	O ₃	9.9	10.0	10.0	9.4
	NO _x	9.8	7.7	10.5	8.9
% missing data for 20-year period	NO	27.6	21.9	15.1	18.1
	NO ₂	11.1	8.6	10.7	9.4
	CO	7.1	8.8	8.0	6.6
	SO ₂	26.7	17.4	9.0	14.1

Monthly mean (Mmean) was calculated from hourly data if 50% or more of the hourly data were available within the month. If this criterion was not fulfilled, the resultant missing monthly data were replaced with median values calculated over a sliding window of length 10 months using “movmedian” function within MATLAB 2019b. In addition to O₃, Mmean was calculated for oxides of nitrogen (NO, NO₂ and NO_x) and selected pollutant ratios such as NO/NO₂, CO/NO_x, and SO₂/NO_x. Monthly mean for daily maximum (Mmax) values were also calculated for O₃ as the daily maximum for the period between 12 p.m. and 6 p.m. if more than 3 h of data were available within a day. The moving median method was also used to replace missing values for Mmax O₃ concentration as required.

Trend analysis on Mmean and Mmax was done using Theil-Sen estimator, which is a non-parametric method that is robust in the presence of outliers and requires little prior information regarding measurement errors [24,25]. The trend analysis was performed in R (version 3.6.2), using the “stl” function in the openair package to deseasonalize the data with Loess smoothing [26]. Loess smoothing applies a weighted least squares method for its polynomial fit and is also robust against presence of outliers [27,28]. Spearman’s Rank-Order Correlation analysis was carried out on the monthly mean (Mmean) values of the pollutants to determine the relationship between O₃ and other gaseous parameters.

Emissions data ranging from 1997 to 2015 for NO_x, CO, and SO₂ were obtained from EDGARv5.0) [29,30]. The data extracted have a yearly temporal resolution and are gridded at horizontal grid spacing of 0.1° × 0.1°. To allow comparison between station point data and EDGAR’s gridded data, the “point-to-pixel comparison” approach [31] was used, whereby the value of the grid where the station point is in was extracted as station data. The number of active vehicles on road by state was obtained from the Road Transport Department of Malaysia [32].

3. Results and Discussion

3.1. Overview of Ozone Distribution

Kuala Lumpur, the capital city of Malaysia, and its surrounding area, the greater Klang Valley region, is a highly dense urban-commercial hub in Malaysia. Station S3 is located within the Klang Valley region and is close to an international shipping port. Station S2 is located north of Kuala Lumpur and the Klang Valley, while stations S1 and S4 are the locations furthest north and south, respectively, from Kuala Lumpur. Distribution of hourly O₃ within the 20-year period for all four of these stations are presented in Figure 2. The mean values were within the range of 18–21 ppb, while the medians were in the range of 11–17 ppb. Stations S1 and S4 show higher median and mean values within the 20-year period compared to stations S2 and S3. The mirror image line on each side of the boxplot shows the distribution of the hourly data as a probability density plot. These so-called violin plots

show some skewness in the distribution, as hourly values at S2 and S3 are more densely populated below the mean. S1 and S4 data also have a higher density of data distributed below the mean, but the probability density plot peak is broader at these two stations. Although the overall density and mean values indicate O₃ concentrations extending to higher values at stations S1 and S4, neither stations recorded the highest observations of O₃, and in fact, S3 recorded the highest hourly O₃ value of 171 ppb, followed by S2 with 158 ppb.

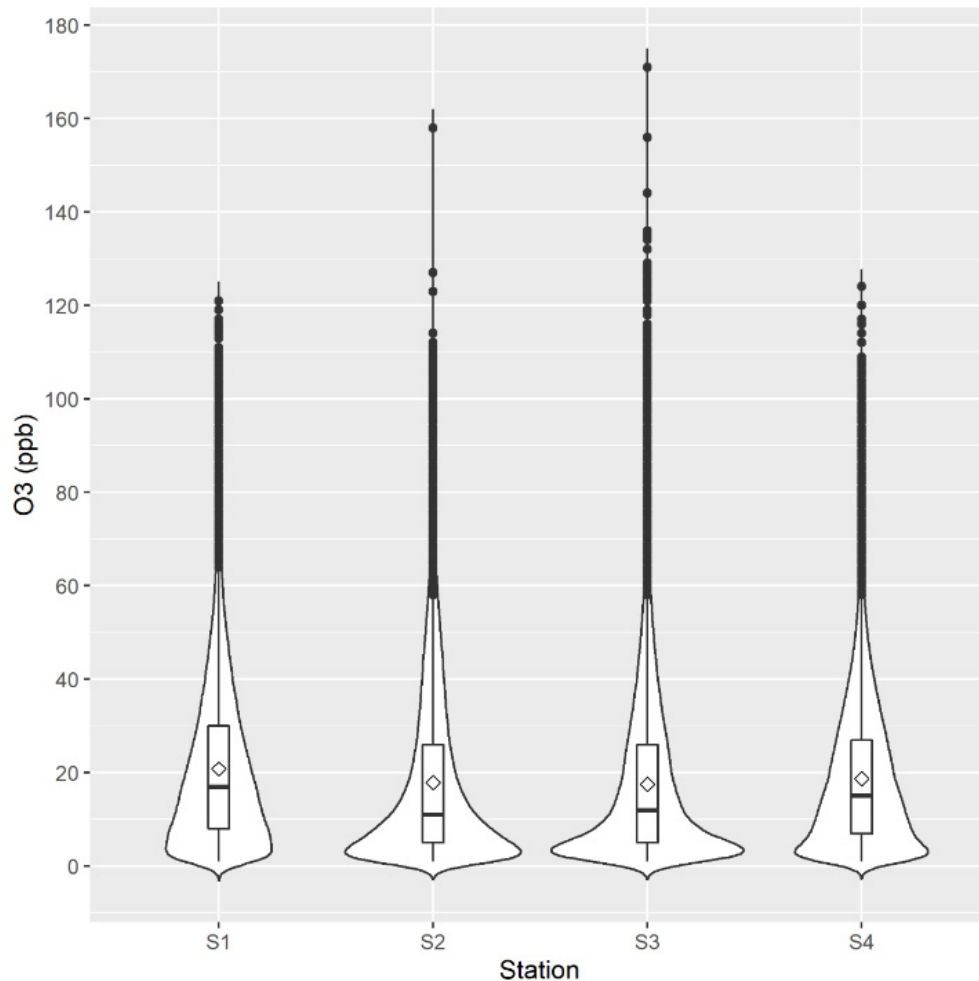


Figure 2. The violin plot provides a mirror image of the probability density function for each station. Box plots are also shown and mean values are labeled with diamond shaped markers.

The ambient air quality standard in Malaysia for hourly O₃ is 100 ppb [33]. Calculation of the fraction of hourly O₃ values higher than this threshold shows that S3 records the highest non-compliance (Figure 3). The station is also the only location to record O₃ non-compliance that is higher in the first decade of the study, while all the other locations show much higher occurrence of non-compliance to O₃ in the latter decade (2007–2016). Time series plots of O₃ Mmean and Mmax are shown in Figure 4a,b, respectively. Most of the monthly mean O₃ readings fall within the range of 10–25 ppb, while the monthly mean of daily maximum O₃ was mostly within the 50–100 ppb range. Mmean at S1 records a much higher occurrence of Mmean falling within the upper range of 25–35 ppb O₃. S3 records the highest occurrence of Mmax falling in the upper range of 100–150 ppb mostly in the earlier part of the decade (1997–2006), consistent with the results of hourly exceedance.

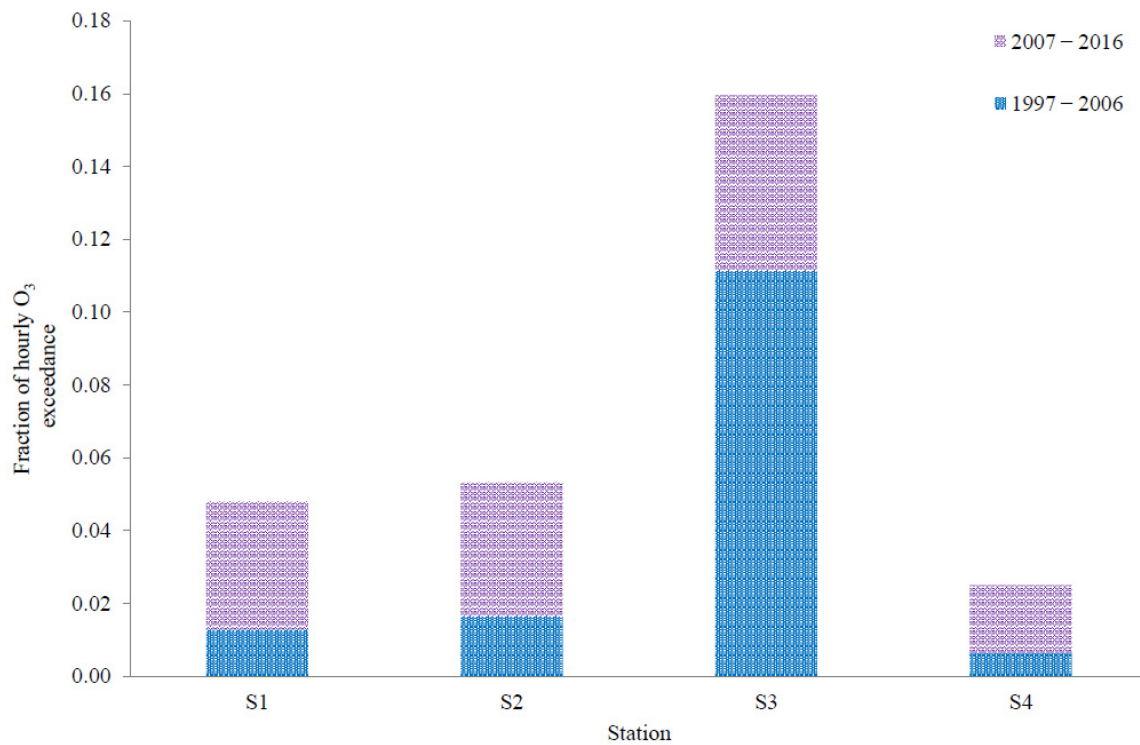


Figure 3. Fraction of hourly O₃ concentrations that were higher than 100 ppb. The fraction is calculated from total hours of O₃ exceedance divided by total available data for each station within the selected period.

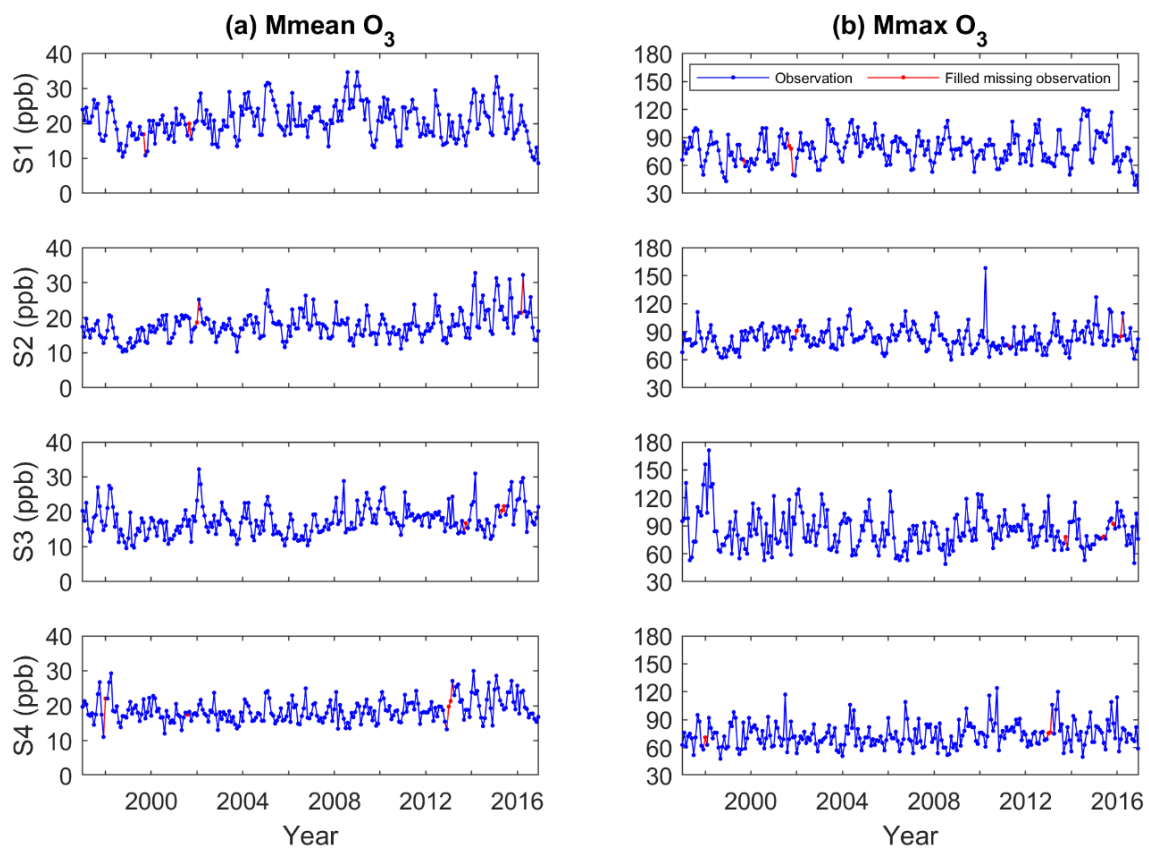


Figure 4. Time series (1997–2016) for (a) Monthly mean O₃ (Mmean) and (b) Monthly mean of daily max O₃ (Mmax).

Although the area around all four stations has been undergoing development within the 20-year period, the locales of stations S2 and, particularly, S3 were already more urbanized compared to S1 and S4 prior to 1997 (Supplementary Figure S1 provides satellite images for the stations during December 1996 and December 2016 for comparison). Station S3 has been shown to be among the locations that record very high O₃ in Peninsular Malaysia [5,6,34]. Hence, the observed higher non-compliance and Mmax values at this location are largely to be expected. The hourly O₃ distribution and Mmean values, however, indicate that the smaller and less densely urbanized areas such as around S1 are showing higher frequency of O₃ concentrations falling in the upper range of the observations. To understand long term trends in O₃ at the monitoring stations and its possible relation to other pollutants such as NO, deseasonalized trends (Section 3.2), correlation (Section 3.3), and diurnal composites (Section 3.4) are analyzed over the 20-year study period as well as for ten year intervals of 1997–2006 and 2007–2016.

3.2. Trends in Ozone, Oxides of Nitrogen, and Selected Pollutant Ratios

Deseasonalized trends for O₃ and selected parameters are presented in Table 2. The Mmean O₃ for the entire study period indicates significant increasing O₃ at S2, S3, and S4 at $p < 0.05$, with rates of 0.19, 0.21, and 0.13 ppb yr⁻¹, respectively. At S1, the trend is much lower, with an increase of only 0.09 ppb yr⁻¹ ($p < 0.10$). Overall, these results correspond to global trends, which show increasing surface and tropospheric O₃ [24,35–40]. Decadal intervals, however, show that not all stations record significant increasing trends of O₃. For the period between 1997 and 2006, only S1 and S2 recorded significant increases in O₃ trends, with S1 recording the highest significant increase (0.51 ppb yr⁻¹) between all stations for all periods studied. Between 2007 and 2016, S1 showed a decreasing O₃ trend instead, at a rate of -0.44 ppb yr⁻¹ ($p < 0.05$), which contributed to it recording the lowest increase in O₃ over the entire 1997–2016 period. Stations S2, S3, and S4, meanwhile, showed significant increasing trends for the period between 2007 and 2016. S4 and S2 recorded the second and third highest rates of O₃ increase with 0.44 and 0.42 ppb yr⁻¹ ($p < 0.05$), respectively, during this period. Although the 20-year trend showed increasing O₃ at all stations, the O₃ trend over the decadal period was less consistent between stations.

Table 2. Deseasonalized trends for monthly mean (Mmean) pollutant concentrations and monthly mean of daily maximum O₃ (Mmax O₃) concentrations.

	1997–2006	2007–2016	1997–2016	1997–2006	2007–2016	1997–2016
	Deseasonalized Mmean O ₃ (ppb yr ⁻¹)			Deseasonalized Mmax O ₃ (ppb yr ⁻¹)		
S1	0.51	-0.44	<i>0.09</i>	1.25	-0.24	0.13
S2	0.36	0.42	0.19	1.06	0.15	0.03
S3	-0.17	<i>0.25</i>	0.21	-1.35	0.33	-0.15
S4	-0.09	0.44	0.13	-0.21	0.38	0.3
	Deseasonalized Mmean NO (ppb yr ⁻¹)			Deseasonalized Mmean NO ₂ (ppb yr ⁻¹)		
S1	0.30	-0.18	0.12	0.20	0.01	0.16
S2	<i>0.07</i>	-0.31	-0.13	0.63	-0.27	0.02
S3	-1.33	-0.62	-0.98	0.06	0.10	-0.01
S4	0.09	0.13	0.39	0.42	0.24	0.21
	Deseasonalized Mmean NOx (ppb yr ⁻¹)			Deseasonalized Mmean NO/NO ₂ (yr ⁻¹)		
S1	0.43	-0.23	0.24	0.01	-0.01	0.00
S2	0.61	-0.44	-0.08	-0.05	-0.01	-0.01
S3	-1.27	-0.47	-0.99	-0.07	-0.02	-0.04
S4	0.54	0.43	0.62	-0.03	-0.01	0.02
	Deseasonalized Mmean CO/NOx (yr ⁻¹)			Deseasonalized Mmean SO ₂ /NOx (yr ⁻¹)		
S1	-4.30	3.95	-1.45	-0.07	0.00	-0.02
S2	-2.18	1.47	-0.23	-0.08	0.00	-0.03
S3	-0.99	0.46	-0.13	-0.02	0.00 *	-0.01
S4	-2.14	0.34	-0.91	-0.05	0.00	-0.02

Note: Significant trends at $p < 0.05$ in bold; Significant trend at $p < 0.10$ in italics. * trend value is -0.0035 yr⁻¹.

Mmean for oxides of nitrogen were also examined for comparison with O₃ trends, since these are pollutants that play an important role in O₃ photochemistry. Photochemical O₃ formation involves a two-step process involving the dissociation of NO₂ in the presence of sunlight [10,12]:



and the reaction of the oxygen atom with oxygen molecules in the presence of a third body (M):



However, the NO from Equation (1) can rapidly react with the O₃, forming NO₂:



Hence, typically, O₃ peaks do not occur until NO concentrations have fallen, as NO can titrate O₃. The NO and NO_x trends over 1997–2016 both show negative trends for S2 and S3 and a non-significant trend for NO₂. S4 shows significant increase in NO, NO₂ and NO_x for all three periods studied. These trends do not consistently correspond to the Mmean O₃ trends either directly or inversely, and this is expected, since O₃ concentrations in ambient air are not solely influenced by O₃ photochemistry. Comparing the differences in Mmean O₃ trends between some of the stations, such as S3 and S4 or S2 and S3 for the period of 1997–2016, gives better insight into the ozone-precursor behavior. The difference in Mmean O₃ trends for the 1997–2016 period is relatively high between S3 and S4, with a value of 0.08 ppb yr⁻¹. However, a smaller difference of 0.02 ppb yr⁻¹ is recorded between S2 and S3. Similarly, S1 and S4 pairing recorded a difference of only 0.04 ppb yr⁻¹ between them. The NO and NO_x trends show that it is only S2 and S3 that record decreasing levels in these species, while S1 and S4 showed increasing trends in both NO and NO_x level. The NO₂ trends for S1 and S4 both show significant increase within a 20-year period at $p < 0.05$, while both S2 and S3 have non-significant trends, even at $p < 0.10$. The distinctive pairing reflects combination of locations that were more urbanized (S2 and S3) or less urbanized (S1 and S4) prior to 1997.

Trends of Mmax O₃ were more varied between stations and between the selected periods compared to Mmean trends. Only S4 shows a significant positive trend in Mmax O₃, despite the increase in O₃ exceedance in the period between 2007–2016 compared to 1997–2006 at S1, S2, and S4. The Mmax O₃ trends were only significant at S4, with a rate of 0.3 ppb yr⁻¹ for the period between 1997 and 2016. Station S3 recorded a non-significant decreasing Mmax O₃ trend between the 1997 and 2016 period, despite recording the highest Mmean trends for the same period. For the first decadal interval of 1997–2006, S3 showed a significant decrease in O₃ maxima at a rate of -1.35 ppb yr⁻¹, while S1 and S2 recorded significant increasing trends. In the latter interval of 2007–2016, none of the stations recorded significant trends. Given that O₃ maxima are more likely linked to localized influence rather than a combination of regional and local precursor distribution and meteorology [41], fewer significant trends in O₃ maxima in comparison to mean O₃ concentrations at the stations can be expected. Although there is an overall global increase in O₃ and regional photochemical production is an important source of O₃ in decadal time scales [42], local emission profiles or saturation of precursor species are sufficiently dominant to influence O₃ trends. It would appear that peak values of O₃ are less dependent upon an expected increase in emission from urban-commercial expansion, but instead reflect a unique chemistry–meteorology combination that varies on a day to day basis.

Ratios of NO/NO₂, CO/NO_x, and SO₂/NO_x were also analyzed, as these can provide some indications as to whether the location is influenced by mobile or point sources. Given that mobile sources typically have higher emissions of CO and NO_x, while point sources have higher SO₂ and NO_x emissions, high SO₂/NO_x paired with low CO/NO_x ratios, for example, could indicate point sources [43–45]. Increasing NO/NO₂ ratios indicate locations closer to traffic emissions [46,47]. The trend for the ratios shows a decrease for all combinations at S2 and S3, despite these stations

showing urban expansion, which is expected to cause an increase in traffic volume (Figure 5a). Figure 5a does, however, highlight the more urbanized profile of stations S2 and S3, with vehicular counts that are a magnitude higher than stations S1 and S4. The total emissions derived from the EDGAR database (Figure 5b–d) also indicate that S3 has the highest emissions from all sources due to its high population, traffic density, and urban-commercial expansion. It also shows that S1 and S2 have a more similar emission profile to each other, unlike the pairing for the number of active vehicles on the road (Figure 5a).

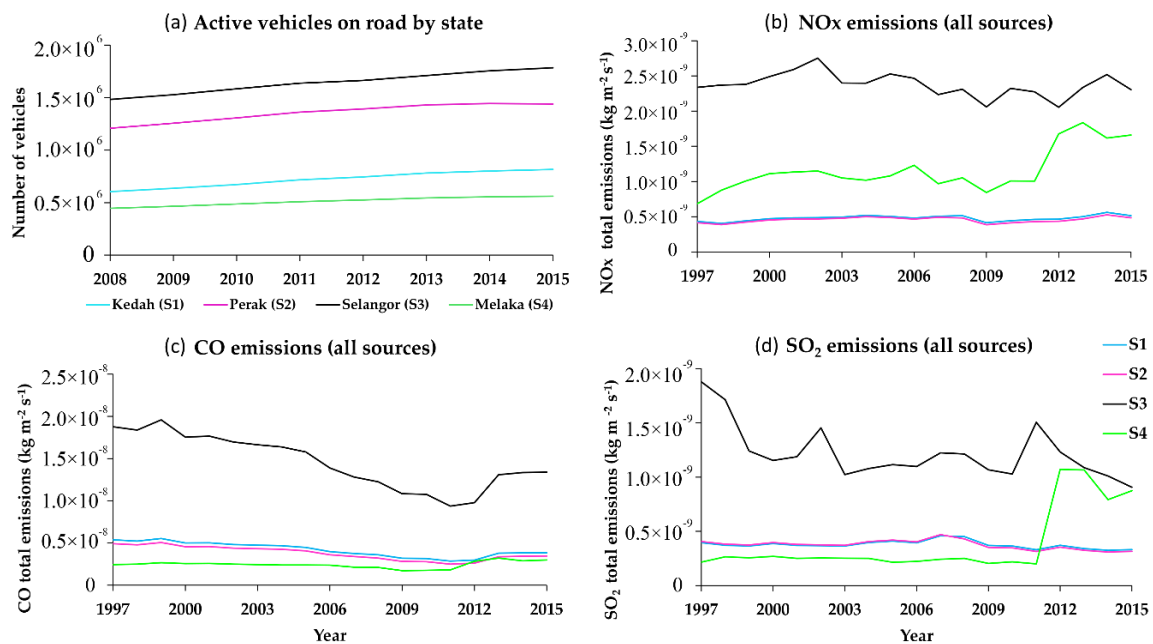


Figure 5. Time series of total active vehicle count by state for the period 2008–2015 (a) and total emissions (all sources) for NOx, CO and SO2 for the period 1997–2015 (a–c).

3.3. Correlation of Monthly Mean Ozone with Selected Parameters

The correlation analysis is carried out on monthly means to smooth out meteorologically influenced diurnal and intra-seasonal signals that could influence O₃ behavior. However, O₃ and other pollutant concentrations are also influenced by emissions, planetary boundary layer height and long-distance transport, in addition to chemistry and meteorology in varying degrees, depending on the time scale chosen [39,48–51]. All of this contributes to the potentially non-linear relationship between O₃ and other pollutants. Hence, a non-parametric method was selected, as the focus is on identifying potential relationship between O₃ and the selected pollutants over the period of study that may provide insight into relative behavior of other pollutants in relation to O₃.

The correlation analysis results between O₃ and selected parameters over the individual decades are shown in Table 3. NO and NO₂ showed negative and positive correlation with O₃, respectively, at all stations with the exception of negative NO₂ correlation with O₃ at S4 for the period between 1997 and 2006. Additionally, data from both S3 and S4 showed insignificant correlation between O₃ and NO at selected durations. Figure 6 presents time series for NO, NO₂, CO, and SO₂, in which S3 records the overall highest pollutant concentrations, while S4 is the only station to show increasing NO in the latter decade. NOx also showed no significant relationship with O₃, except for S4 in the first decade and S3 for the total study duration. With the exception of NO/NO₂ ratios, none of the parameters showed a similar significant relationship between stations when the results were compared between the decadal and total study duration. These results are similar to the trend results, supporting our finding that there is no clear link between ambient O₃ and oxides of nitrogen observations when the results are seen individually.

Table 3. Spearman’s Rank-Order Correlation of Mmean O₃.

		NO	NO ₂	NO _x	NO/NO ₂	CO/NO _x	SO ₂ /NO _x
1997–2006							
S1	O ₃	−0.28	0.27	−0.17	−0.5	0.12	−0.04
S2		−0.46	0.64	0.33	−0.69	−0.19	−0.34
S3		−0.17	0.43	0.04	−0.34	0.44	0.22
S4		−0.41	−0.07	−0.25	−0.22	0.26	0.29
2007–2016							
S1	O ₃	−0.23	0.25	0.02	−0.39	−0.06	0.12
S2		−0.55	0.38	0.01	−0.67	0.09	−0.07
S3		−0.37	0.36	−0.05	−0.52	0.18	0.07
S4		−0.16	0.29	0.08	−0.4	0.18	0.02
1997–2016							
S1	O ₃	−0.18	0.27	−0.01	−0.43	−0.03	−0.04
S2		−0.51	0.5	0.11	−0.69	−0.06	−0.24
S3		−0.38	0.36	−0.18	−0.50	0.29	−0.04
S4		−0.04	0.18	0.04	−0.14	0.12	0.01

Note: Significant correlation at $p < 0.05$ in bold.

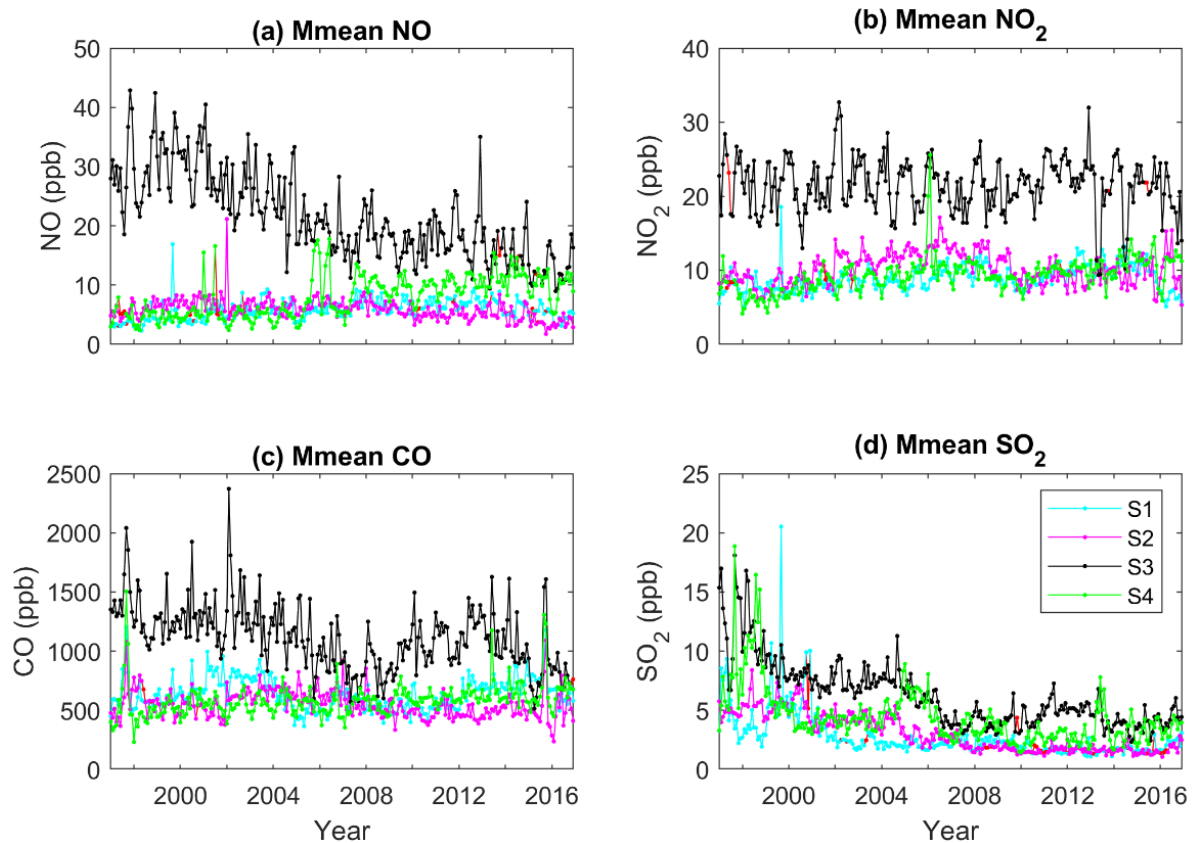


Figure 6. Time series of Mmean for NO (a), NO₂ (b), CO (c), and SO₂ (d). Data points in red are missing observations that have been filled with computed values.

All the stations showed a significant negative relationship with NO/NO₂ ratios, that is, less O₃ at higher NO levels. S2, for example, consistently obtained coefficient values above 0.5 within all study periods for O₃ relationship with NO/NO₂ ratios. O₃ relationship with NO and NO₂ (Equations (1)–(3)) at steady state can be represented by $O_3 = j_{NO_2} [NO_2]/k_1 [NO]$, where j_{NO_2} is the photolysis rate for NO₂ and k_1 is the rate constant for the reaction between NO and O₃ [11]. Hence, the results are in

fact more consistent with control of monthly mean O_3 levels by increasing titration of O_3 by NO into NO_2 . The S1 station had shown a large difference in O_3 trends between the first decade and the last decade. However, results of the correlation analysis do not show large differences in the NO, NO_2 , and NO/ NO_2 relationship with O_3 between the decades. The only observable difference is in the trend of NO itself (Table 2), where NO is increasing in the first decade and decreasing in the next. Without additional information on other precursor species, such as VOC and localized emission profile, it is not possible to determine with certainty if O_3 titration caused the significant change in O_3 in the last few years of the latter decade. The CO/ NO_x and SO_2/NO_x ratios only showed a significant relationship with O_3 at S2, S3, and S4 for the first decade and were not significant during other periods. The lack of consistency in O_3 and pollutant ratio relationship is also reflected in the differing trends of O_3 and pollutant ratio between stations (Table 2).

3.4. Diurnal Variation Composites

In order to determine if there are any changes in the diurnal profile between the decadal intervals at each station, a composite of hourly data was plotted for the period of 1997–2006 and 2007–2016 (Figure 7). The difference between the two (the latter decade minus the earlier decade) was also plotted. The decadal diurnal composites show a change in magnitude of pollutant concentration but no temporal shift (peaks occurring at similar times). O_3 shows an increase at all stations, with S3 showing the largest difference between the decades overall. NO at S2 shows a relatively small decrease in the latter decade compared to S3 that records the largest decrease in NO in the same period. S1 and S4 show an increase in NO, but with an almost similar magnitude of change to S2 and S3, respectively. NO_2 shows a much smaller decadal difference between all the stations compared to NO and hence, the NO/ NO_2 differences are primarily influenced by the change in NO rather than NO_2 . The change in NO, either an increase or decrease, makes only a relatively small difference to NO_2 levels. At S3, which is highly urbanized, the observations suggest that NO to NO_2 conversion (Equation (3)) and O_3 levels are controlled by local NO emissions. At S3, O_3 increases in the latter decade, while NO decreases over the same period. This is consistent with S3 being situated close to NO emission sources and strong titration of O_3 by NO. However, NO to NO_2 conversion can also be affected by formation of NO_2 via the VOC pathway. In contrast to station S3, station S4 shows increase in O_3 and increase in NO between the decades, which is consistent with increased production of NO_2 via reactions of peroxy radicals with NO, e.g., $HO_2/RO_2 + NO \rightarrow OH/RO + NO_2$ [10,52]. Different stations appear to show different NO_x sensitivity and presumably, VOC sensitivity. Having stations with different NO_x and VOC sensitivities poses additional challenge in air pollution mitigation as reduction in NO_x , for example, could actually result in increasing O_3 at some locations such as S3.

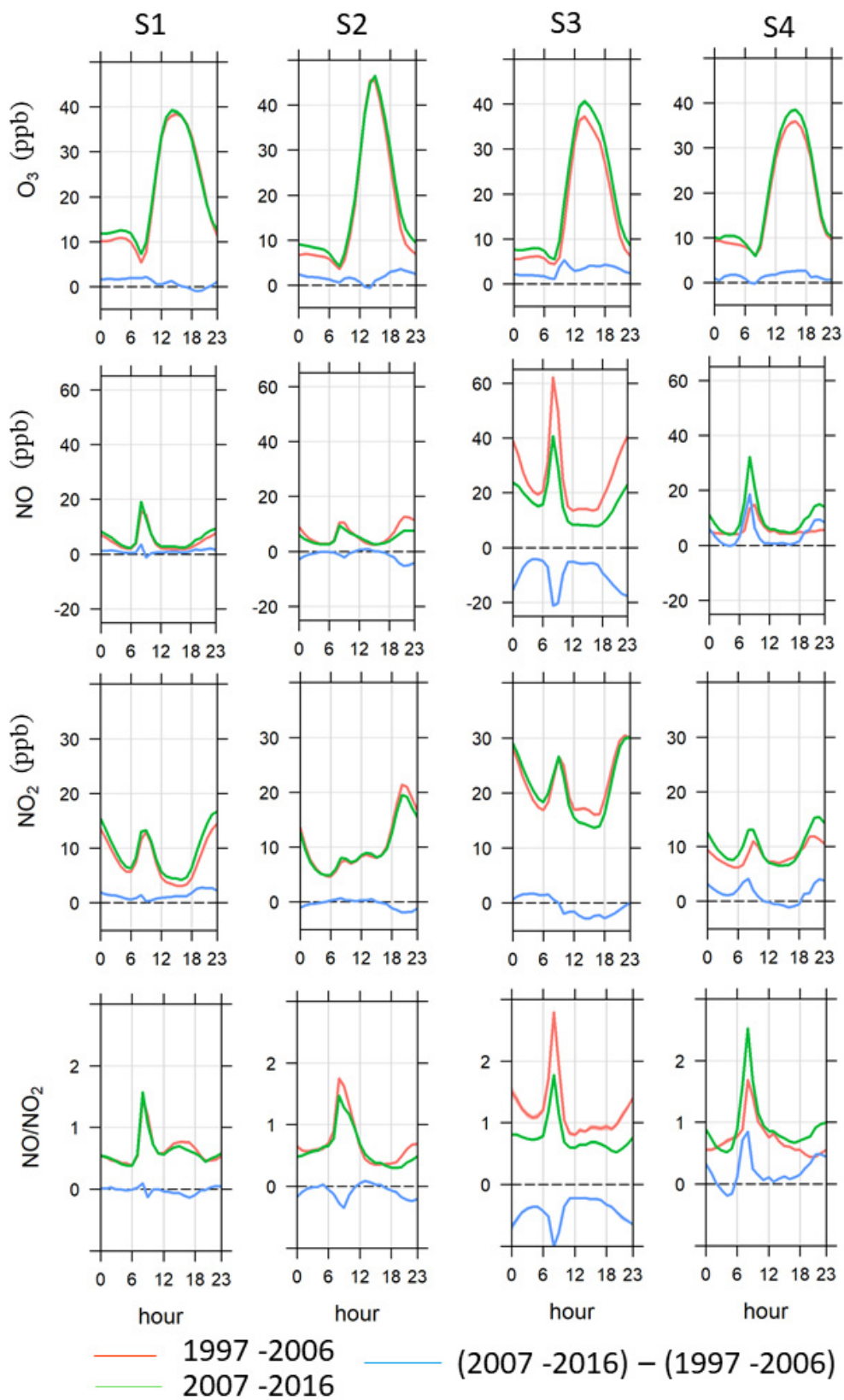


Figure 7. Composite of diurnal plots for O₃, NO, NO₂, and NO/NO₂.

4. Conclusions

The trends in deseasonalized Mmean O₃ show that there has been an increase in O₃ within the 20-year period at all the stations. Station S3, which is the most densely populated and urbanized location, recorded the highest rate of increase (0.21 ppb yr⁻¹, $p < 0.05$). This is followed by stations S2 and S4 at rates of 0.19 and 0.13 ppb yr⁻¹ ($p < 0.05$), respectively. The lowest increase in O₃ was recorded at S1, with a rate of 0.09 ppb yr⁻¹ ($p < 0.10$). Decadal intervals showed a more varied pattern in O₃ trends. In the first decade (1997–2006), S1 showed the highest recorded significant increase in O₃ (0.51 ppb yr⁻¹), but it then recorded the largest significant decrease in O₃ in the 2007–2016 period (−0.44 ppb yr⁻¹). S2 and S4 showed the largest increment over the latter decade (2007–2016), with rates of 0.42 and 0.44 ppb yr⁻¹, respectively. Both the NO and NO_x trends were negative at S2 and S3, while S1 and S4 showed positive trends ($p < 0.05$) during the 1997–2016 period. Mmax O₃ trends were only significant at S4 within the 20-year period (0.3 ppb yr⁻¹). Correlation analysis showed that the NO/NO₂ ratio more consistently produced a significant negative correlation with Mmean O₃ irrespective of the period of analysis, which corresponds to O₃ control by photostationary state reactions. The diurnal composites for decadal changes suggest that the stations may have different NO_x and VOC sensitivities. However, further analysis on O₃ sensitivity to NO_x and VOC is required for conclusive evidence on the potential saturation of NO_x or VOC at the locations.

Supplementary Materials: The following are available online at <http://www.mdpi.com/2073-4433/11/7/755/s1>, Figure S1: Satellite image of station locations in December 1996 and December 2016.

Author Contributions: Conceptualization, F.A.; Data curation, F.A., P.T.G., C.J.X.; Formal analysis, F.A.; writing—original draft preparation, F.A.; writing—review and editing, F.A., P.T.G., M.T.L., L.J., C.J.X.; visualization, F.A., C.J.X.; funding acquisition, F.A. All authors have read and agreed to the published version of the manuscript.

Funding: This research was funded by Universiti Kebangsaan Malaysia, Geran Galakan Penyelidik Muda GGPM-2017-083.

Acknowledgments: The authors would like to thank the DoE Malaysia for the provision of air quality data used in this study.

Conflicts of Interest: The authors declare no conflict of interest. The funders had no role in the design of the study; in the collection, analyses, or interpretation of data; in the writing of the manuscript, or in the decision to publish the results.

References

1. Fleming, Z.L.; Doherty, R.; von Schneidmesser, E.; Malley, C.; Cooper, O.; Pinto, J.; Colette, A.; Xu, X.; Simpson, D.; Schultz, M.; et al. Global Ozone Distribution relevant to Human Health: Metrics and present day levels from the Tropospheric Ozone Assessment Report (TOAR). *Elem. Sci. Anth.* **2018**, *6*. [[CrossRef](#)]
2. Pleijel, H.; Broberg, M.C.; Uddling, J.; Mills, G. Current surface ozone concentrations significantly decrease wheat growth, yield and quality. *Sci. Total Environ.* **2018**, *613*, 687–692. [[CrossRef](#)] [[PubMed](#)]
3. Ishii, S.; Bell, J.; Marshall, F. Phytotoxic risk assessment of ambient air pollution on agricultural crops in Selangor State, Malaysia. *Environ. Pollut.* **2007**, *150*, 267–279. [[CrossRef](#)]
4. Wan Mahiyuddin, W.R.; Sahani, M.; Aripin, R.; Latif, M.T.; Thach, T.-Q.; Wong, C.-M. Short-term effects of daily air pollution on mortality. *Atmos. Environ.* **2013**, *65*, 69–79. [[CrossRef](#)]
5. Latif, M.T.; Huey, L.S.; Juneng, L. Variations of surface ozone concentration across the Klang Valley, Malaysia. *Atmos. Environ.* **2012**, *61*, 434–445. [[CrossRef](#)]
6. Mohtar, A.A.A.; Latif, M.T.; Baharudin, N.H.; Ahamad, F.; Chung, J.X.; Othman, M.; Juneng, L. Variation of major air pollutants in different seasonal conditions in an urban environment in Malaysia. *Geosci. Lett.* **2018**, *5*, 21. [[CrossRef](#)]
7. Azmi, S.Z.; Latif, M.T.; Ismail, A.S.; Juneng, L.; Jemain, A.A. Trend and status of air quality at three different monitoring stations in the Klang Valley, Malaysia. *Air Qual. Atmos. Health* **2010**, *3*, 53–64. [[CrossRef](#)]
8. Latif, M.T.; Othman, M.; Idris, N.; Juneng, L.; Abdullah, A.M.; Hamzah, W.P.; Khan, M.F.; Nik Sulaiman, N.M.; Jewaratnam, J.; Aghamohammadi, N.; et al. Impact of regional haze towards air quality in Malaysia: A review. *Atmos. Environ.* **2018**, *177*, 28–44. [[CrossRef](#)]

9. Keywood, M.; Ayers, G.; Gras, J.; Boers, C. Haze in the Klang valley of Malaysia. *Atmos. Chem. Phys. Discuss.* **2003**, *3*, 615–653. [[CrossRef](#)]
10. Finlayson-Pitts, B.J.; Pitts, J.N. *Chemistry of the Upper and Lower Atmosphere: Theory, Experiments and Applications*; Academic Press: San Diego, CA, USA, 2000.
11. Seinfeld, J.H.; Pandis, S.N. *Atmospheric Chemistry and Physics: From Air Pollution to Climate Change*, 2nd ed.; John Wiley and Sons, Inc.: New York, NY, USA, 2006.
12. Sillman, S. The relation between ozone, NO_x and hydrocarbons in urban and polluted rural environments. *Atmos. Environ.* **1999**, *33*, 1821–1845. [[CrossRef](#)]
13. Chameides, W.; Fehsenfeld, F.; Rodgers, M.; Cardelino, C.; Martinez, J.; Parrish, D.; Lonneman, W.; Lawson, D.; Rasmussen, R.; Zimmerman, P. Ozone precursor relationships in the ambient atmosphere. *J. Geophys. Res.* **1992**, *97*, 6037–6055. [[CrossRef](#)]
14. Lu, X.; Zhang, L.; Chen, Y.; Zhou, M.; Zheng, B.; Li, K.; Liu, Y.; Lin, J.; Fu, T.M.; Zhang, Q. Exploring 2016–2017 surface ozone pollution over China: Source contributions and meteorological influences. *Atmos. Chem. Phys.* **2019**, *19*, 8339–8361. [[CrossRef](#)]
15. Ellis, A.W.; Hildebrandt, M.L.; Thomas, W.M.; Fernando, H. Analysis of the climatic mechanisms contributing to the summertime transport of lower atmospheric ozone across metropolitan Phoenix, Arizona, USA. *Clim. Res.* **2000**, *15*, 13–31. [[CrossRef](#)]
16. Banan, N.; Latif, M.T.; Juneng, L.; Ahamad, F. Characteristics of Surface Ozone Concentrations at Stations with Different Backgrounds in the Malaysian Peninsula. *Aerosol Air Qual. Res.* **2013**, *13*, 1090–1106. [[CrossRef](#)]
17. Toh, Y.Y.; Lim, S.F.; Von Glasow, R. The influence of meteorological factors and biomass burning on surface ozone concentrations at Tanah Rata, Malaysia. *Atmos. Environ.* **2013**, *70*, 435–446. [[CrossRef](#)]
18. Ismail, M.; Suroto, A.; Ismail, N.A. Time series analysis of surface ozone monitoring records in Kemaman, Malaysia. In *Air Pollution—A Comprehensive Perspective*; Haryanto, B., Ed.; InTechOpen: London, UK, 2012. [[CrossRef](#)]
19. Ashfold, M.; Latif, M.; Samah, A.; Mead, M.I.; Harris, N.R. Influence of Northeast Monsoon cold surges on air quality in Southeast Asia. *Atmos. Environ.* **2017**, *166*, 498–509. [[CrossRef](#)]
20. Awang, N.R.; Ramli, N.A.; Shith, S.; Zainordin, N.S.; Manogaran, H. Transformational characteristics of ground-level ozone during high particulate events in urban area of Malaysia. *Air Qual. Atmos. Health* **2018**, *11*, 715–727. [[CrossRef](#)]
21. Awang, N.R.; Ramli, N.A.; Shith, S.; Md Yusof, N.F.F.; Zainordin, N.S.; Sansuddin, N.; Ghazali, N.A. Time effects of high particulate events on the critical conversion point of ground-level ozone. *Atmos. Environ.* **2018**, *187*, 328–334. [[CrossRef](#)]
22. Latif, M.T.; Dominick, D.; Ahamad, F.; Khan, M.F.; Juneng, L.; Hamzah, F.M.; Nadzir, M.S.M. Long term assessment of air quality from a background station on the Malaysian Peninsula. *Sci. Total Environ.* **2014**, *482*, 336–348. [[CrossRef](#)]
23. Jamaluddin, A.F.; Tangang, F.; Chung, J.X.; Juneng, L.; Sasaki, H.; Takayabu, I. Investigating the mechanisms of diurnal rainfall variability over Peninsular Malaysia using the non-hydrostatic regional climate model. *Meteorol. Atmos. Phys.* **2018**, *130*, 611–633. [[CrossRef](#)]
24. Wang, T.; Dai, J.; Lam, K.S.; Nan Poon, C.; Brasseur, G.P. Twenty-Five Years of Lower Tropospheric Ozone Observations in Tropical East Asia: The Influence of Emissions and Weather Patterns. *Geophys. Res. Lett.* **2019**, *46*, 11463–11470. [[CrossRef](#)]
25. Fernandes, R.G.; Leblanc, S. Parametric (modified least squares) and non-parametric (Theil–Sen) linear regressions for predicting biophysical parameters in the presence of measurement errors. *Remote Sens. Environ.* **2005**, *95*, 303–316. [[CrossRef](#)]
26. Carslaw, D.C.; Ropkins, K. openair—An R package for air quality data analysis. *Environ. Modell. Softw.* **2012**, *27–28*, 52–61. [[CrossRef](#)]
27. Cleveland, R.B.; Cleveland, W.S.; McRae, J.E.; Terpenning, I. STL: A seasonal-trend decomposition. *J. Off. Stat.* **1990**, *6*, 3–73.
28. Bigi, A.; Ghermandi, G.; Harrison, R.M. Analysis of the air pollution climate at a background site in the Po valley. *J. Environ. Monit.* **2012**, *14*, 552–563. [[CrossRef](#)]

29. Crippa, M.; Oreggioni, G.; Guizzardi, D.; Muntean, M.; Schaaf, E.; Lo Vullo, E.; Solazzo, E.; Monforti-Ferrario, F.; Olivier, J.; Vignati, E. *Fossil CO₂ and GHG Emissions of All World Countries*; Publication Office of the European Union: Luxembourg, 2019.
30. EDGAR v5.0 Global Air Pollutant Emissions. Available online: https://edgar.jrc.ec.europa.eu/overview.php?v=50_AP (accessed on 23 June 2020). [[CrossRef](#)]
31. Tan, M.L.; Samat, N.; Chan, N.W.; Roy, R. Hydro-meteorological assessment of three GPM satellite precipitation products in the Kelantan River Basin, Malaysia. *Remote Sens.* **2018**, *10*, 1011. [[CrossRef](#)]
32. Number of Vehicles On The Road by State, Malaysia, 2008–2015. Available online: http://www.data.gov.my/data/ms_MY/dataset/bilangan-kenderaan-di-atas-jalan-rama-mengikut-negeri (accessed on 21 June 2020).
33. *Laporan Kualiti Alam Sekeliling 2016 (Environmental Quality Report)*; Department of Environment Malaysia: Putrajaya, Malaysia, 2017.
34. Awang, N.R.; Elbayoumi, M.; Ramli, N.A.; Yahaya, A.S. Diurnal variations of ground-level ozone in three port cities in Malaysia. *Air Qual. Atmos. Health* **2016**, *9*, 25–39. [[CrossRef](#)]
35. Cooper, O.R.; Parrish, D.; Ziemke, J.; Balashov, N.; Cupeiro, M.; Galbally, I.; Gilge, S.; Horowitz, L.; Jensen, N.; Lamarque, J.-F.; et al. Global distribution and trends of tropospheric ozone: An observation-based review. *Elem. Sci. Anth.* **2014**, *2*, 000029. [[CrossRef](#)]
36. Anet, J.G.; Steinbacher, M.; Gallardo, L.; Velásquez Álvarez, P.A.; Emmenegger, L.; Buchmann, B. Surface ozone in the Southern Hemisphere: 20 years of data from a site with a unique setting in El Tololo, Chile. *Atmos. Chem. Phys.* **2017**, *17*, 6477–6492. [[CrossRef](#)]
37. Nair, P.R.; Ajayakumar, R.S.; David, L.M.; Girach, I.A.; Mottungan, K. Decadal changes in surface ozone at the tropical station Thiruvananthapuram (8.542° N, 76.858° E), India: Effects of anthropogenic activities and meteorological variability. *Environ. Sci. Pollut. Res.* **2018**, *25*, 14827–14843. [[CrossRef](#)]
38. Fu, Y.; Liao, H.; Yang, Y. Interannual and decadal changes in tropospheric ozone in China and the associated chemistry-climate interactions: A review. *Adv. Atmos. Sci.* **2019**, *36*, 975–993. [[CrossRef](#)]
39. Guicherit, R.; Roemer, M. Tropospheric ozone trends. *Chemosphere Glob. Chang. Sci.* **2000**, *2*, 167–183. [[CrossRef](#)]
40. Assareh, N.; Prabamroong, T.; Manomaiphobon, K.; Theramongkol, P.; Leungsakul, S.; Mitrjit, N.; Rachiwong, J. Analysis of observed surface ozone in the dry season over Eastern Thailand during 1997–2012. *Atmos. Res.* **2016**, *178–179*, 17–30. [[CrossRef](#)]
41. Ahamad, F.; Latif, M.T.; Tang, R.; Juneng, L.; Dominick, D.; Juahir, H. Variation of surface ozone exceedance around Klang Valley, Malaysia. *Atmos. Res.* **2014**, *139*, 116–127. [[CrossRef](#)]
42. Nagashima, T.; Sudo, K.; Akimoto, H.; Kurokawa, J.; Ohara, T. Long-term change in the source contribution to surface ozone over Japan. *Atmos. Chem. Phys.* **2017**, *17*, 8231–8246. [[CrossRef](#)]
43. Parrish, D.D.; Trainer, M.; Buhr, M.P.; Watkins, B.A.; Fehsenfeld, F.C. Carbon monoxide concentrations and their relation to concentrations of total reactive oxidized nitrogen at two rural U.S. sites. *J. Geophys. Res. Atmos.* **1991**, *96*, 9309–9320. [[CrossRef](#)]
44. Aneja, V.P.; Agarwal, A.; Roelle, P.A.; Phillips, S.B.; Tong, Q.; Watkins, N.; Yablonsky, R. Measurements and analysis of criteria pollutants in New Delhi, India. *Environ. Intern.* **2001**, *27*, 35–42. [[CrossRef](#)]
45. Goyal, P. Present scenario of air quality in Delhi: A case study of CNG implementation. *Atmos. Environ.* **2003**, *37*, 5423–5431. [[CrossRef](#)]
46. Coppalle, A.; Delmas, V.; Bobbia, M. Variability of NO_x and NO₂ concentrations observed at pedestrian level in the city centre of a medium sized urban area. *Atmos. Environ.* **2001**, *35*, 5361–5369. [[CrossRef](#)]
47. Mavroidis, I.; Ilija, M. Trends of NO_x, NO₂ and O₃ concentrations at three different types of air quality monitoring stations in Athens, Greece. *Atmos. Environ.* **2012**, *63*, 135–147. [[CrossRef](#)]
48. Zhang, J.; Ouyang, Z.; Miao, H.; Wang, X. Ambient air quality trends and driving factor analysis in Beijing, 1983–2007. *J. Environ. Sci.* **2011**, *23*, 2019–2028. [[CrossRef](#)]
49. Gardner, M.W.; Dorling, S.R. Meteorologically adjusted trends in UK daily maximum surface ozone concentrations. *Atmos. Environ.* **2000**, *34*, 171–176. [[CrossRef](#)]
50. Vingarzan, R. A review of surface ozone background levels and trends. *Atmos. Environ.* **2004**, *38*, 3431–3442. [[CrossRef](#)]

51. Pusede, S.E.; Steiner, A.L.; Cohen, R.C. Temperature and recent trends in the chemistry of continental surface ozone. *Chem. Rev.* **2015**, *115*, 3898–3918. [[CrossRef](#)]
52. Manahan, S.E. *Fundamentals of Environmental Chemistry*; CRC Press: Boca Raton, FL, USA, 2011.



© 2020 by the authors. Licensee MDPI, Basel, Switzerland. This article is an open access article distributed under the terms and conditions of the Creative Commons Attribution (CC BY) license (<http://creativecommons.org/licenses/by/4.0/>).